Progress In Electromagnetics Research, Vol. 146, 187–194, 2014

Experimental Realization of Strong DC Magnetic Enhancement with Transformation Optics

Kexin Liu[1], Wei Jiang[1], Fei Sun[1, 2], and Sailing He[1, 2, *]

(*Invited Paper*)

Abstract—A passive DC magnetic concentrator is designed with transformation optics (TO) and realized by meta-materials. The passive DC magnetic concentrator based on space compression transformation can greatly enhance the magnetic field in a free space region and can be used for e.g., improving the sensitivity of magnetic sensors and increasing the efficiency of wireless energy transmission. The magnetic property of the medium obtained by TO is extremely anisotropic. To solve this, we use magnetic metamaterials made of alternated high-permeability ferromagnetic (HPF) materials and high-temperature superconductor (HTS) materials. We optimize our structure by conducting simulations using the finite element method (FEM) and experimentally demonstrate a strong, 4.74-time enhancement of the DC magnetic field by our meta-material magnetic concentrator. We also demonstrate that a simplified structure with only HPF materials working at room temperature can still gives 3.84-time enhancement of the DC magnetic field. The experimental results are in good agreement with the numerical simulations based on FEM.

1. INTRODUCTION

Achieving stronger static or quasi-static magnetic fields in a specific region will give rise to a revolution in many technical applications, including improving the sensitivity of magnetic sensors [1], increasing the efficiency of wireless energy transmission [2], improving the resolution of magnetic resonance imaging (MRI) [3], promoting the manipulation of drug delivery using magnetic nano-particles [4, 5], etc. Besides using active magnets with extremely high power consumption to achieve stronger fields [6], we can use passive magnetic lenses or concentrators that can cause an external magnetic field to converge without consuming additional power to obtain enhanced DC magnetic fields in a specific region [7–9].

Many different kinds of DC magnetic lenses or concentrators have been proposed. One type is designed with ferromagnetic materials. However, the enhancing performances of these ferromagnetic devices are limited by saturation magnetization [7]. Another type that has been designed and experimentally demonstrated is based on superconductors with a high critical field H_c [8, 9]. However, those devices based on purely superconductors can only achieve an enhanced DC magnetic field in a very small free region with a very low enhancement factor (e.g., about 2 or 3 times). Furthermore, those superconductor magnetic lenses lack systematic theoretical guidance on how to design the desired enhancement of magnetic fields [8, 9].

In recent years, transformation optics (TO) based on the invariance form of Maxwell's equations [10, 11] has become a powerful theoretical tool. A special medium (often referred to as the

Received 27 April 2014, Accepted 22 May 2014, Scheduled 4 June 2014
Invited paper for the Commemorative Collection on the 150-Year Anniversary of Maxwell's Equations.
* Corresponding author: Sailing He (sailing@jorcep.org).
[1] Centre for Optical and Electromagnetic Research, Zhejiang Provincial Key Laboratory for Sensing Technologies, JORCEP (Sino-Swedish Joint Research Center of Photonics), Zhejiang University, Hangzhou 310058, China. [2] Department of Electromagnetic Engineering, School of Electrical Engineering, Royal Institute of Technology (KTH), Stockholm S-100 44, Sweden.

transformed medium), which can control the trace of the electromagnetic wave (e.g., perfect lens [12] and electromagnetic cloaks [13]) and also the static electric or magnetic field [14–20], can be designed by TO. As the transformed medium is often complex, which may not exist in nature, people have to design some artificial materials (e.g., meta-materials) to create them. Very recently, a concentrating and transmitting device for DC magnetic energy based on TO is realized by meta-materials [21]. However, the 2.70-time enhancement of the magnetic field is still weak. It needs a very large area to get a stronger enhancement due to the limitation of the TO method they used [17]. In this paper we use a different space compression method [20] to experimentally realize a magnetic concentrator with the same cross-section area as in [21], but with a much stronger enhancement of the magnetic field. In Section 2, we will describe the design method and give numerical simulation results based on the finite element method (FEM). In Section 3, we will construct the actual magnetic concentrator made of meta-materials consisting of both high-permeability ferromagnetic (HPF) materials and high-temperature superconductor (HTS) materials. The experimental setups and results of measurements will also be shown. In Section 4, we will give a summary and further discussion.

2. DESIGN METHOD

2.1. DC Magnetic Concentrator Designed by TO

Our aim is to design a practical passive magnetic concentrator to concentrate the external applied magnetic field in an inner free region, where sensors can be placed. The method we use is space compression transformation [22, 23], which has been used for optical energy concentration. For simplicity, we consider a two-dimensional (2D) structure. As shown in Fig. 1, different colors stand for different regions. In the reference space, or virtual space, (Fig. 1(a)), all regions are free spaces whatever colors are used. In the real space (Fig. 1(b)), we have different permeability media (i.e., transformed media) in different colored regions. The red region in the reference space is compressed into the red region in the real space, and thus the DC magnetic field will be enhanced in that region. The green regions and yellow regions have also been correspondingly transformed from the reference space to the real space. In the grey region, we choose an identical transformation, which means the grey region in the real space is still free space.

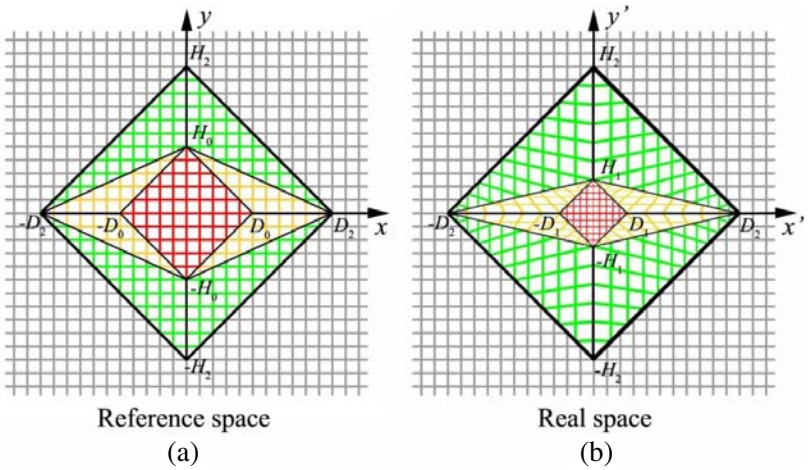

Figure 1. The transformation relations between the reference space and the real space. Red, yellow and green regions in each quadrant are correspondingly transformed from the reference space to the real space. Grey regions do not change through the transformation.

The corresponding medium in each region in the real space has been calculated using TO in our previous work [20]. Since we deal with static magnetic field in a 2D system, the static magnetic field only has components in the x'-y' plane, so that only the left-upper 2×2 matrix of the permeability tensor has some physical relevance. This is different from the electromagnetic wave case shown in reference [22],

which requires both the permeability tensor and permittivity tensor. By choosing the following proper geometrical parameters of our device:

$$\begin{aligned} D_1 = H_1 = \alpha D_0 = \alpha H_0 \\ D_2 = H_2 = \beta D_0 = \beta H_0 \end{aligned} \tag{1}$$

the corresponding 2×2 matrices of the permeability tensors in each colored region in the real space take the following forms:

$$\overline{\overline{\mu}}_{yellow} = \mu_0 \begin{bmatrix} \dfrac{(\beta-\alpha)^2 + \beta^2(\alpha-1)^2}{\alpha(\beta-1)(\beta-\alpha)} & -sign(x')sign(y')\beta\dfrac{\alpha-1}{\beta-\alpha} \\ -sign(x')sign(y')\beta\dfrac{\alpha-1}{\beta-\alpha} & \dfrac{\beta-1}{\beta-\alpha}\alpha \end{bmatrix} \tag{2}$$

$$\overline{\overline{\mu}}_{green} = \mu_0 \begin{bmatrix} \dfrac{\beta-1}{\beta-\alpha} & -sign(x')sign(y')\dfrac{\alpha-1}{\beta-\alpha} \\ -sign(x')sign(y')\dfrac{\alpha-1}{\beta-\alpha} & \dfrac{(\alpha-1)^2+(\beta-\alpha)^2}{(\beta-1)(\beta-\alpha)} \end{bmatrix} \tag{3}$$

$$\overline{\overline{\mu}}_{red} = \mu_0 \mathrm{diag}(1,1) \tag{4}$$

From Eqs. (1) and (4), the red region is a square, and the transformed medium in the red region just reduces to air. Even though the red region is transformed, the medium in the red region is still air (unlike the electromagnetic wave case [22]).

In the principal axis system (ξ-χ coordinate system), permeability tensor becomes diagonal:

$$\begin{bmatrix} \mu_{x'x'} & \mu_{x'y'} \\ \mu_{x'y'} & \mu_{y'y'} \end{bmatrix} \overset{\text{coordinate system rotates}}{\longrightarrow} \mathrm{diag}(\mu_{\xi\xi}, \mu_{\chi\chi})$$

where

$$\begin{aligned} \mu_{\xi\xi} &= \cos^2\theta\mu_{x'x'} + \sin^2\theta\mu_{y'y'} + 2\sin\theta\cos\theta\mu_{x'y'} \\ \mu_{\chi\chi} &= \sin^2\theta\mu_{x'x'} + \cos^2\theta\mu_{y'y'} - 2\sin\theta\cos\theta\mu_{x'y'} \end{aligned} \tag{5}$$

$$\theta = \frac{1}{2}\arctan\left(\frac{2\mu_{x'y'}}{\mu_{x'x'} - \mu_{y'y'}}\right) \tag{6}$$

Here θ is the rotation angle between the ξ-χ system and the x'-y' system (see the insert of Fig. 2(a)).

In order to achieve an effect of DC magnetic field concentration, α and β should satisfy that $0 < \alpha < 1$ and $\beta > 1$. As the field in the red region with size D_0 in the reference space is compressed into the field in the red region with size $D_1 = \alpha D_0$ in the real space, the compression ratio of the space is α and the enhancement of the field is simply $1/\alpha$. Moreover, from Eq. (4), the red region in the real space is still a free space where we can put our magnetic sensor. Taking the limit $\beta \to \infty$ in Eqs. (2) and (3), we can obtain:

$$\overline{\overline{\mu}}_{yellow,\beta\to\infty} = \mu_0 \begin{bmatrix} \dfrac{1+(\alpha-1)^2}{\alpha} & -sign(x')sign(y')(\alpha-1) \\ -sign(x')sign(y')(\alpha-1) & \alpha \end{bmatrix} \tag{7}$$

$$\overline{\overline{\mu}}_{green,\beta\to\infty} = \mu_0 \mathrm{diag}(1,1) \tag{8}$$

Eq. (8) indicates that the medium in the green region in the real space will approach free space when β approaches infinity. In practice, we can omit the green region to reduce the size of our DC magnetic concentrator. In addition, $\beta \to \infty$ theoretically requires the device to be infinitely long along the x' direction. In practice, we can choose a relatively long length along x' direction (the size of the device is finite) to approximate this requirement. Furthermore, in order to get a strong enhancement, we take the limit $\alpha \to 0$ in Eq. (7) and substitute the result to Eqs. (5) and (6), and we obtain

$$\overline{\overline{\mu}}_{yellow,\alpha\to0,\beta\to\infty} = \mathrm{diag}(\mu_{\xi\xi} \to \infty, \mu_{\chi\chi} \to 0) \tag{9}$$

$$\theta_{\alpha\to0,\beta\to\infty} = 0 \tag{10}$$

Note that if $\alpha \to 0$, it means that the enhancement is infinitely large. However, from Eq. (9), this means that the magnetic property of the medium in yellow region is extremely anisotropic (infinite in one direction and zero in another orthogonal direction), which cannot exist in natural materials. To solve this issue, we use magnetic meta-materials made of alternated HPF materials (with very large permeability) and HTS materials (with very small permeability) to approximate the theoretical requirement. As a result, we can only obtain a finite enhancement factor and the rotation angle θ is not exactly zero. The rotation angle needs to be optimized by simulations. In addition, to make a comparison with the results in [21], the structure that we design has the same cross-section area as the structure in [21].

2.2. Numerical Simulation

The 3D simulations are obtained by FEM of the AC/DC module in the Comsol Multiphysics software [24]. Figs. 2(a) and 2(b) show, respectively, the front view and diametric view of the designed meta-material magnetic concentrator. The inner free space is a square with $R_1 = 9.4\,\text{mm}$, and the outer meta-material structure is a rectangle with $R_2 = 75\,\text{mm}$. The length L in the x direction is 70 mm. The HPF pieces (blue line) and HTS pieces (grey line) are alternatively displaced. The thickness of the HPF pieces is 0.15 mm, and the permeability of them is set as diag (1E3, 1, 1E3) in their principle coordinates. Given that the superconductor layers in HTS pieces are about only 1 μm thick and possess almost total diamagnetism in one direction, in order to run the simulation effectively and correctly, the thickness of the superconductor pieces is set to be 0.2 mm and the permeability of them set as diag (1,1E-2,1) in their principle coordinates. The non-magnetic gaps between HPF pieces and HTS pieces are 1 mm each. The rotation angle θ optimized by simulations is 5 degrees. The enhancement of the magnetic field is defined by the ratio of the B_z field component in the center to the uniform applied field B_a. The simulated B_z/B_a field component is plotted in planes IN and OUT as shown in Fig. 3(a). The enhancement is 4.81, and the field is relatively uniform in the inner free space.

We also study if a simplified structure of the metamaterial can give similar concentration results. Since the use of HTS pieces requires cryogenics which may limit the applicability of the device, we calculate the performance of a structure with only HPF pieces at room temperatures ($T = 300\,\text{K}$) above the critical temperature T_c of the superconductors, at which the HTS pieces are deactivated. An

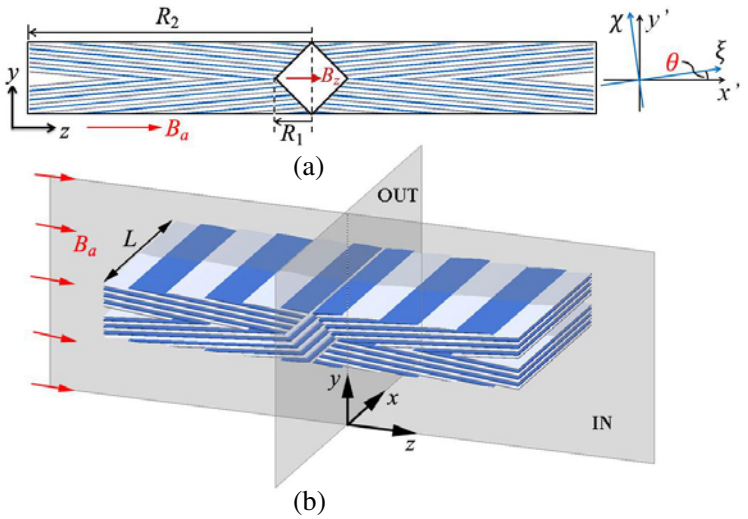

Figure 2. Sketch of the meta-material magnetic concentrator. (a) Front view. The inner free space is a square with $R_1 = 9.4\,\text{mm}$ and the outer meta-material structure is a rectangle with $R_2 = 75\,\text{mm}$. The HPF pieces (blue line) and HTS pieces (grey line) are alternately displaced. The white gaps between them are non-magnetic. The insert on the right shows the rotation angle θ between the ξ-χ system and the x'-y' system. The rotation angle θ optimized by simulations is 5 degrees. (b) Diametric view. The length L in the x direction is 70 mm. The magnetic field B_a is applied along the z direction.

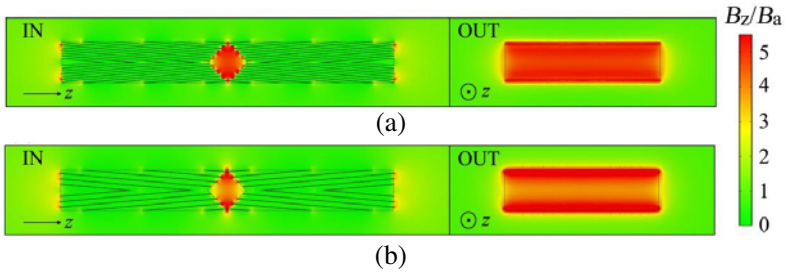

Figure 3. Results of simulations. The simulated B_z/B_a field component is plotted in planes IN and OUT (illustrated in Fig. 2(b)). (a) For the case of HPF pieces alternated with HTS pieces (i.e., $T < T_c$), the enhancement at the center is 4.81, and the field is relatively uniform in the inner free space. (b) For the case of only HPF pieces (i.e., $T = 300\,\mathrm{K} > T_c$), the enhancement at the center is 3.88.

enhancement of 3.88 can still be achieved, although the magnetic field distribution in the inner space is not uniform. The simulated B_z/B_a field of the simplified magnetic concentrator is plotted in planes IN and OUT as shown in Fig. 3(b).

3. EXPERIMENTS

3.1. Meta-Material Magnetic Concentrator

We use commercial HPF pieces and HTS pieces to fabricate our meta-material magnetic concentrator illustrated in Fig. 2. The HPF pieces are Co-NETIC® AA (an alloy of Fe and Ni) from the Magnetic Shield Corporation. They are 0.15 mm thick and cut into 70 mm long rectangles whose widths are determined by the lengths of the blue lines in Fig. 2(a). The HTS pieces are made of Amperium® copper laminated wire (containing ceramic films of yttrium-barium-copper-oxide) from the American Superconductor Corporation [25]. The wire is 12 mm wide, 0.2 mm thick, and cut into 70 mm long strips. Several strips are parallel-fixed with adhesive tape with proper overlaps to make HTS pieces

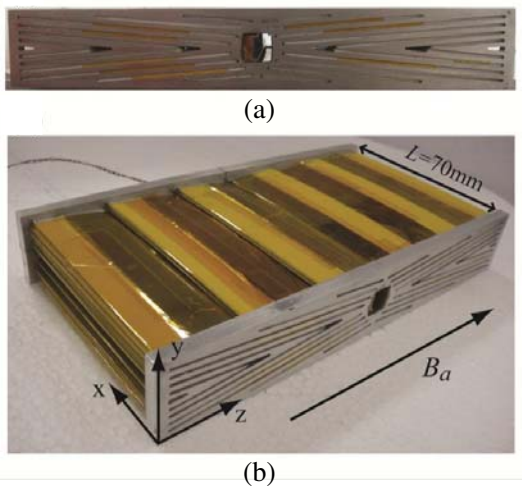

Figure 4. Photos of our real meta-material magnetic concentrator. The HPF pieces and the HTS pieces are fixed on 1 mm thick and 80 mm long plastic boards by Kapton tapes, and then the edges of the plastic boards are inserted into specific slots in two aluminum support plates The slots in the aluminum plates with depth of 5 mm and width of 1 mm are used to ensure appropriate placement of HPF and HTS pieces. A Hall sensor is located at the center of the inner free space through the square hole by an aluminum slab. (a) Front view. (b) 3D view.

whose widths are the lengths of the grey lines in Fig. 2(a). To ensure the appropriate placement of HPF pieces and HTS pieces, they are fixed on 1 mm thick and 80 mm long plastic boards by Kapton® tapes, and then the edges of plastic boards are inserted into specific slots with depth of 5 mm and width of 1 mm in two aluminum support plates. Figs. 4(a) and 4(b) illustrate, respectively, the front view and 3D view of the fabricated meta-material magnetic concentrator. A uniform magnetic field will be applied along the z direction. A magnetic sensor can be located at the center of the inner free space through the square hole by an aluminum slab.

3.2. Experimental Setups and Results

The Helmholtz coils used to generate a uniform applied field B_a have a radius of 180 mm and are aligned and separated by a distance of 180 mm. Our magnetic concentrator is placed in the central region of the Helmholtz coils. A Hall sensor (Lakeshore HGCT-3020) is located at the center of the inner free space to measure the B_z field component. A 100 mA constant current is supplied to the Hall sensor by a Keithley 2400 sourcemeter. The Hall voltage is measured by a $6^{1/2}$-digit multimeter (34410A) from Agilent. The measurement below T_c is done by submerging the concentrator and the Hall sensor into liquid nitrogen ($T = 77$ K). The experiments are performed both at 77 K and at room temperature ($T = 300$ K). Fig. 5(a) and Fig. 5(b) show the experimental setups to measure the magnetic field enhancements at 77 K and 300 K, respectively. The measured field B_z at the center of the inner free space is plotted as a function of the magnetic field B_a generated by the coils (at 77 K and 300 K) in Fig. 5(c). The corresponding linear fits are presented in dashed lines whose slopes are 4.74 and 3.84 for 77 K (red) and 300 K (blue), together with simulations results presented in solid lines whose slopes are 4.81 and 3.88 for 77 K (red) and 300 K (blue), respectively. The results demonstrate a strong enhancement of the magnetic field in the central free space of the meta-material magnetic concentrator.

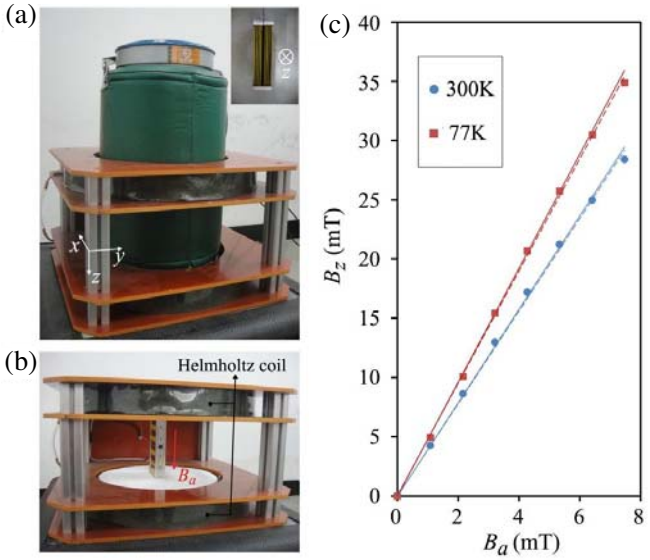

Figure 5. Experimental setups and results. The Helmholtz coils used to generate a uniform applied field B_a along the z direction have a radius of 180 mm and are aligned and separated by a distance of 180 mm. Our magnetic concentrator is placed in the central region of the Helmholtz coils. A Hall sensor is located at the center of the inner free space to measure the B_z field component. (a) The experimental setup at 77 K. The magnetic concentrator and the Hall sensor are submerged into liquid nitrogen as shown in the insert. The green tank containing liquid nitrogen is non-magnetic. (b) The experimental setup at 300 K. (c) The measured field B_z at the center of the inner free space is plotted as a function of the applied field B_a for the case at 77 K (red square) and the case at 300 K (blue circle). The corresponding linear fits are presented in dashed lines whose slopes are 4.74 and 3.84 for 77 K (red) and 300 K (blue), together with simulation results presented in solid lines whose slopes are 4.81 and 3.88 for 77 K (red) and 300 K (blue), respectively.

4. SUMMARY AND DISCUSSION

We have designed a passive DC magnetic concentrator via space compression transformation. A reduction method ($\alpha \to 0$, $\beta \to \infty$) has been used to simplify and realize such a concentrator. The concentrator has been optimized by simulations using FEM and realized by meta-materials consisting of alternated HPF pieces and HTS pieces. The experimental results have demonstrated a strong, 4.74-time enhancement of the DC magnetic field by our meta-material magnetic concentrator. Compared with the device in [21], our magnetic concentrator possesses a much stronger enhancement of the magnetic field, although they have the same cross-section area. The results are obtained by using commercially available materials and at liquid-nitrogen temperatures, indicating that our idea might have applications such as improving the sensitivity of magnetic sensors, increasing the efficiency of wireless energy transmission and improving the resolution of MRI. We have also shown that a further simplified structure with only HPF pieces, working at room temperature can still enhance the magnetic field with a slight decrease in the performance (still giving an enhancement factor of 3.84). There is still room to improve the magnetic field enhancement of our device. If we increase the length of the device along x' direction to satisfy better the theoretical requirement, the enhancement can be improved. We can also use better ferromagnetic materials (with higher permeability and stronger saturation magnetization) and better cooling technology (providing lower temperature) to improve the performance of our device. When extending the device from DC to a low frequency band, we may use a combination of ferromagnetic materials and metamaterials without superconductors to realize it.

ACKNOWLEDGMENT

This work is partially supported by the National High Technology Research and Development Program (863 Program) of China (No. 2012AA030402), the National Natural Science Foundation of China (Nos. 61178062 and 60990322), the Program of Zhejiang Leading Team of Science and Technology Innovation, Swedish VR grant (# 621-2011-4620) and SOARD. Fei Sun thanks the China Scholarship Council (CSC) No. 201206320083.

REFERENCES

1. Ripka, P. and M. Janosek, "Advances in magnetic field sensors," *IEEE Sens. J.*, Vol. 10, No. 6, 1108–1116, 2010.
2. Kurs, A., A. Karalis, R. Moffatt, J. D. Joannopoulos, P. Fisher, and M. Soljacic, "Wireless power transfer via strongly coupled magnetic resonances," *Science*, Vol. 317, No. 5834, 83–86, 2007.
3. Brown, M. A. and R. C. Semelka, *MRI: Basic Principles and Applications*, Wiley-Blackwell, 2010.
4. Veiseh, O., J. W. Gunn, and M. Zhang, "Design and fabrication of magnetic nanoparticles for targeted drug delivery and imaging," *Advanced Drug Delivery Reviews*, Vol. 62, No. 3, 284–304, 2010.
5. Dobson, J., "Magnetic micro- and nano-particle-based targeting for drug and gene delivery," *Nanomedicine*, Vol. 1, No. 1, 31–37, 2006.
6. National High Magnetic Field Laboratory, http://www.magnet.fsu.deu/usershub/scientificdivisions /dcfield/facilities.html.
7. Iwasa, Y., "Hybrid magnets: A magnet engineer's experience and a proposal for the next generation of hybrids," *Physica B*, Vol. 216, Nos. 3–4, 1996.
8. Kiyoshi, T., S. Choi, S. Matsumoto, T. Asano, and D. Uglietti, "Magnetic flux concentrator using Gd-Ba-Cu-O bulk superconductors," *IEEE Transactions on Applied Superconductivity*, Vol. 19, No. 3, 2174–2177, 2009.
9. Zhang, Z. Y., S. Choi, S. Matsumoto, R. Teranshi, G. Giunchi, A. F. Albisetti, and T. Kiyoshi, "Magnetic lenses using different MgB2 bulk superconductors," *Supercond. Sci. Technol.*, Vol. 25, No. 2, 025009, 2012.
10. Leonhardt, U. and T. G. Philbin, *Geometry and Light: Science of Invisibility*, Dover, 2010.

11. Pendry, J. B., D. Schurig, and D. R. Smith, "Controlling electromagnetic fields," *Science*, Vol. 312, No. 5781, 1780–1782, 2006.
12. Pendry, J. B., "Negative refraction makes a perfect lens," *Physical Review Letters*, Vol. 85, No. 18, 3966–3969, 2000.
13. Schurig, D., J. J. Mock, B. J. Justice, S. A. Cummer, J. B. Pendry, A. F. Starr, and D. R. Smith, "Metamaterial electromagnetic cloak at microwave frequencies," *Science*, Vol. 314, No. 5801, 977–980, 2006.
14. Yang, F., Z. L. Mei, T. Y. Jin, and T. J. Cui, "DC electric invisibility cloak," *Physical Review Letters*, Vol. 109, 053902, 2012.
15. Gömöry, F., M. Solovyov, J. Šouc, C. Navau, J. Prat-Camps, and A. Sanchez, "Experimental realization of a magnetic cloak," *Science*, Vol. 335, No. 6075, 1466–1468, 2012.
16. Narayana, S. and Y. Sato, "DC magnetic cloak," *Advanced Materials*, Vol. 24, No. 1, 71–74, 2012.
17. Navau, C., J. Prat-Camps, and A. Sanchez, "Magnetic energy harvesting and concentration at a distance by transformation optics," *Physical Review Letters*, Vol. 109, 263903, 2012.
18. Sun, F. and S. He, "Create a uniform static magnetic field over 50T in a large free space region," *Progress In Electromagnetics Research*, Vol. 137, 149–157, 2013.
19. Sun, F. and S. He, "Static magnetic field concentration and enhancement using magnetic materials with positive permeability," *Progress In Electromagnetics Research*, Vol. 142, 579–590, 2013.
20. Sun, F. and S. He, "DC magnetic concentrator and omnidirectional cascaded cloak by using only one or two homogeneous anisotropic materials of positive permeability," *Progress In Electromagnetics Research*, Vol. 142, 683–699, 2013.
21. Prat-Camps, J., C. Navau, and A. Sanchez, "Experimental realization of magnetic energy concentration and transmission at distance by metamaterials," arXiv: 1308.5878, 2013.
22. Rahm, M., D. Schurig, D. A. Roberts, S. A. Cummer, D. R. Smith, and J. B. Pendry, "Design of electromagnetic cloak and concentrators using form-invariant coordinate transformations of Maxwell's equations," *Photonics and Nanostructures-fundamentals and Applications*, Vol. 6, 87–95, 2008.
23. Li, W., J. Guan, and W. Wang, "Homogeneous-materials-constructed electromagnetic field concentrators with adjustable concentrating ratio," *J. Phys. D: Appl. Phys.*, Vol. 44, 125401, 2011.
24. The Finite Element Simulation is Conducted by Using Commercial Software COMSOL Multiphysics, http://www.comsol.com.
25. Rupich, M. W., X. Li, S. Sathyamurthy, C. L. H. Thieme, K. DeMoranville, J. Gannon, and S. Fleshler, "Second generation wire development at AMSC," *IEEE Transactions on Applied Superconductivity*, Vol. 23, No. 3, 6601205, 2013.